

Abiotic Controls on H₂ Production from Basalt—Water Reactions and Implications for Aquifer Biogeochemistry

TODD O. STEVENS* AND
JAMES P. MCKINLEY

Pacific Northwest National Laboratory, P.O. Box 999,
Richland, Washington 99352

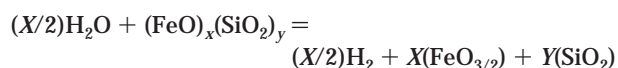
Abiotic production of H₂ from basalt reactions in aqueous solutions is hypothesized to support microbial ecosystems in deep subsurface aquifers, such as those found in the Columbia River Basalt group (CRB). We investigated factors controlling this phenomenon, including rock composition, pH, temperature, sterilization method, reducing agents, and product removal. Ferrous silicate minerals were found to be the basalt components responsible for H₂ production from anaerobic water–rock interactions. H₂ evolution was faster at pH < 7 but occurred from pH 5 to pH 11, which covers the pH range (7–10) measured in CRB groundwaters. The onset of H₂ evolution coincided with the appearance of dissolved Fe²⁺, and an apparent alkaline inhibition could be alleviated by the addition of excess FeCl₂. This may reflect, in part, the low redox conditions needed for H₂ evolution and suggests that H₂ may be controlled by reaction rates of ferrous silicate minerals. Rates were higher at 60 °C than at 30 °C, suggesting that the geothermal gradient may lead to increased H₂ production at depth. The results were consistent with the hypothesis that basalt–redox reactions support primary production by microorganisms in some terrestrial subsurface environments.

Introduction

Dissolved H₂ is found in groundwaters around the world at concentrations ranging from less than 1 nM to many micromolar (1–8). In anaerobic microbial communities, H₂ serves as an important metabolic currency (9), and diverse chemolithoautotrophic microorganisms can use H₂ as an electron donor in the production of organic matter from dissolved inorganic carbon (DIC) (e.g., ref 10). Thus, where environmental conditions permit, H₂-bearing waters might support the primary production of organic matter in subsurface microbial communities (8, 11–14). Such a phenomenon could have important implications for the evolution of the earth's biosphere and for potential biospheres elsewhere (14–16). In addition, many microorganisms can couple the oxidation of H₂ to the reductive transformation of various organic and inorganic compounds that are potential threats to public health and environmental quality (17–20), so that understanding the origin of reduced gases in the subsurface could aid in predicting the distribution and fate of those substances in the environment. Finally, because H₂ can sometimes reach high enough concentrations

to form a safety hazard itself (21), it may be important to understand its formation in groundwater.

The occurrence of elevated H₂ in the subsurface has been reported to result from a variety of abiotic processes. Some of these processes could be important to broad-based energy budgets for microbes in the subsurface, but their relative importance is poorly understood. Near zones of active volcanism, H₂ might enter groundwaters from mantle outgassing or water–magma interactions (e.g., refs 22 and 23). Where groundwater flows through ultramafic rocks, H₂ can be added to solution as a product of serpentinization, which involves the reduction of water and sometimes CO₂ by reduced iron during weathering (24, 25). For example, for the reaction of an arbitrary ferrous silicate with water:



Although the exact reaction pathway and stoichiometry are not well-constrained, this reaction may be adapted, by the inclusion of appropriate constant-valence metal–oxide components, to describe the production of H₂ from water reacting with any silicate mineral containing an FeO component. Serpentinization is well-known at elevated temperatures, e.g., near seafloor spreading centers (26), but considerable evidence has also been published for low-temperature serpentinization in continental groundwater settings (1, 2). The release of H₂ during fracturing of quartz (e.g., as might occur ephemerally during an earthquake) has also been attributed to reaction of water with surface Si–O radicals created by mechanical disruption of crystal lattices (27). Alternatively, the evolution of H₂ during the fracturing of igneous and metamorphic rocks in the laboratory has been attributed to the incorporation of small amounts of water (in the form of OH[−]) into the structure of nominally anhydrous minerals that crystallize from H₂O-laden melts. Subsequent *in situ* redox conversion of OH[−] pairs to peroxy anions plus H₂ could be followed by the diffusion of H₂ to the mineral surface or grain boundary and later liberation during fracturing (28).

In addition to abiotic H₂ generation, well-known biotic sources can contribute H₂ directly or indirectly to groundwaters. Where buried organic matter is present, H₂ might arise from microbial fermentation. Concentrations of H₂ greater than a few nanomolar are not common in sedimentary fermentation-based communities because of consumption by hydrogenotrophic organisms. However, considerably higher concentrations occur in environments such as intestinal tracts or landfills that are not electron-donor limited (29–31). Thermal decomposition of buried organic matter primarily yields CH₄, although significant H₂ might be produced under extreme conditions, such as magmatic contact, or possibly by the subsequent corrosion of metallic iron generated from ferrous or ferric minerals during such an encounter (32).

We have been investigating a microbial ecosystem within tholeiitic Columbia River Basalts of Miocene Age, in the northwestern United States, which we hypothesize is based on the *in situ* production of H₂ from interactions of groundwater with basalt (8). The H₂ is thought to serve as an electron donor for primary production by aquifer microorganisms, including methanogens. Basalts are, in general, less reducing than ultramafic rocks and contain lower concentrations of ferrous iron. However, the observation of micromolar and higher H₂ in CRB groundwaters (8, 33), the production of explosive H₂ concentrations during drilling

* Corresponding author e-mail: todd.stevens@pnl.gov; phone: (509)373-0891; fax: (509)376-1321.

through CRB clasts (21), and the production of H_2 in laboratory experiments (8) led us to hypothesize that redox reactions between ferrous iron-containing silicates and water also produce H_2 in basaltic environments. Some of the other mechanisms listed above are unlikely. For instance, active volcanism and native iron, required for thermogenic H_2 or H_2 generated by the reaction of zero-valent iron with water are not known in the CRB. A recent publication (34) argued that CH_4 in the CRB aquifers originated from the fermentation of organic matter and that the H_2 observed in basalt-groundwater microcosms in the laboratory originated from the silica-radical mechanism of Kita et al. (27). However, that paper (34) contained no evidence to substantiate those claims and no observations of or experiments with CRB materials. Isolated minor occurrences of organic matter can be found in the CRB. For instance, two thin interbeds in our study area contain coal-like material, and occasional petrified trees still contain some charcoal-like material. However, as described elsewhere (8, 35), geochemical trends observed in basin-wide groundwater samples indicate that methane is formed from the reduction of CO_2 with H_2 . Here we report new evidence on the factors affecting the evolution of H_2 from basalts and demonstrate that significant amounts of this gas can be generated under conditions prevailing in the CRB.

Materials and Methods

Samples and Sample Preparation. Unless otherwise stated, basalt samples were obtained from a reference outcrop of known composition, designated Reference Umtanum Col-lonade (RUC) (36). The mineral composition of this sample was as follows: plagioclase, 36.2%; pyroxene, 18.1%; glassy mesostasis, 38.2%; titaniferous magnetite, 4.6%; apatite, 0.98%; and alteration products, 0.31%. Uncharacterized hand samples were also obtained from outcrops of various basalt flows, exposed by erosion, along the Columbia River in central Washington. Specimens of several individual mineral phases were obtained from Ward's Earth Science, Rochester, NY.

All samples were pulverized to produce relatively high surface areas. This was to allow laboratory-scale experiments of feasible size and duration. It was important to ensure that tiny chips of steel from the processing equipment did not contaminate the sample, since H_2 is readily produced by corrosion of the Fe^0 found in tool steel, and steel tools are readily eroded by hard rock. Magnetically separated fines from the finished product were examined microscopically and by X-ray diffraction to detect any Fe^0 contamination. Initially, basalt samples were excavated and reduced to centimeter-sized rubble, using other pieces of basalt as tools; however, we found that use of ordinary soft-metal sledge hammers did not result in detectable Fe^0 contamination and produced similar experimental results. (We found that mechanical jaw-crushers, even though all working surfaces were ceramic, did not perform acceptably. Although initial samples were free of contamination, mechanical wear of internal mechanisms eventually shed steel fragments into the samples.) After visibly weathered fragments were removed, samples were milled in a ceramic ball mill (U.S. Stoneware, Akron, OH) or with a large mortar and pestle. Both methods yielded a surface area of approximately $1\text{ m}^2\text{ g}^{-1}$, measured by the BET N_2 -adsorption method.

Sterilization of Basalt Samples. Unless otherwise noted, samples were sterilized by autoclaving two times at 121°C and 2 bar for 20 min on successive days. In one experiment to compare sterilization methods, samples were alternatively sterilized by dry heat at 200°C for 4 h. Aliquots of both autoclaved and baked samples were re-milled overnight in sterile ball mills to regenerate fresh surfaces. Sterility was evaluated by plating subsamples from each treatment on tryptic soy-broth agar plates.

Hydrogen-Production Assays. Aliquots of milled rock, generally 5 g unless specified otherwise, were placed in Balch-type anaerobic culture tubes (Bellco Glass, Vineland, NJ) and sterilized under loose foil covers. Tubes were then sealed with sterile butyl rubber stoppers and flushed with high-purity N_2 from which trace contaminants were removed with an Aeronex (San Diego, CA) "gatekeeper" filtration unit and sterile $0.2\text{-}\mu\text{m}$ pore-sized filter cartridges. (The standard heated copper catalyst system used to remove trace O_2 for anaerobic culture work was found to add unacceptable amounts of H_2 to the experiment.) Negative controls contained 5 g of clean Iota quartz sand.

Experiments were initiated by injecting 5 mL of sterile anaerobic solution through the stopper with a hypodermic needle and refilling the headspace with N_2 , while venting, to achieve 1 bar of N_2 headspace. Solutions consisted of 25 mM PIPES (pH 5–7) or 25 mM borax (pH 7–11) buffers, as specified for each experiment. The pH of experimental solutions was measured during each sampling event, to ensure that it had not changed during incubation. Where experiments were amended with other solutes, they were added from concentrated, sterile, anaerobic stock solutions with a hypodermic needle at time zero. Samples were incubated at 30°C , unless noted otherwise, and separate sets of four tubes were sampled for each time point by removing 1 mL of headspace with a gas-tight syringe after vigorous shaking. Tubes were not resampled, except where the headspace was refilled with N_2 , as noted below. Concentrations of H_2 were determined by gas chromatography with a Trace Analytical (Menlo Park, CA) RGA-3 mercury-reduction detector system. When necessary, headspace samples were diluted with known volumes of purified N_2 , and unused dilution blanks were used to measure background concentrations of H_2 in the dilution gas, which were typically near or below the detection limit.

Results and Discussion

Sterile unweathered basalt surfaces reacted with anaerobic water to produce H_2 as shown in Figures 1–3. No H_2 was produced in the presence of O_2 , in the absence of water, or in the absence of basalt. Consequently, those control data are not shown in the figures. There was considerable variability in the rate and amount of H_2 produced from different basalt flows (data not shown). Even within single flows, different cooling features produced different amounts of H_2 . For instance, the center of a basalt "pillow" yielded severalfold more H_2 than the glassier material near the edge. This suggested that the mineral composition of the basalt, which varies between and within flows, particularly with respect to ferrous iron concentration and phase, could have a controlling influence on surrounding dissolved H_2 concentrations.

To identify the H_2 -producing reactive components, specimen samples of several primary mineral phases common in basalt were obtained, tested for H_2 -generating ability, and analyzed for composition. These minerals are formally grouped according to their crystallographic and chemical properties and included olivine, pyroxene, and feldspar. The nominal stoichiometry of each mineral of interest was as follows: olivine, $(Mg,Fe)_2(SiO_4)$; pyroxene, $(Ca,Mg,Fe)_2Si_2O_6$; and (plagioclase) feldspar, $(Ca,Na)(Al,Si)AlSi_3O_8$ (where the elements in parentheses may freely substitute for one another). Each group is divided arbitrarily into a subset of named minerals based on a limited compositional range within a "solid solution series" where the series is defined by free isomorphic substitution between two elements (e.g., Fe and Mg) within the crystal lattice. The mineral names and nominal formulas for the specimen minerals we used were olivine: forsterite, Mg_2SiO_4 ; olivine: fayalite, Fe_2SiO_4 ; (clino)pyroxene: augite, $Ca(Mg,Fe)Si_2O_6$; and plagioclase feldspar: labo-

TABLE 1. Composition of Enriched Mineral Phases Shown in Figure 1^a

mineral	SiO ₂	Al ₂ O ₃	CaO	FeO	MgO	Na ₂ O	K ₂ O	sum
forsterite	41.97	0.20	0.12	7.23	38.88	0.00	0.00	88.4
fayalite	29.75	0.00	—	64.60	1.5	—	—	99.2
augite	53.96	1.91	18.90	8.80	11.43	1.65	0.28	96.9
labradorite	54.79	25.74	10.41	2.34	1.10	4.97	0.43	99.8

^a Labradorite composition was determined by acid digestion followed by ICP-AES. Ferrous silicate compositions were by electron microprobe analysis of polished mounts. Both methods used mineral standards. Dashes represent components not quantified.

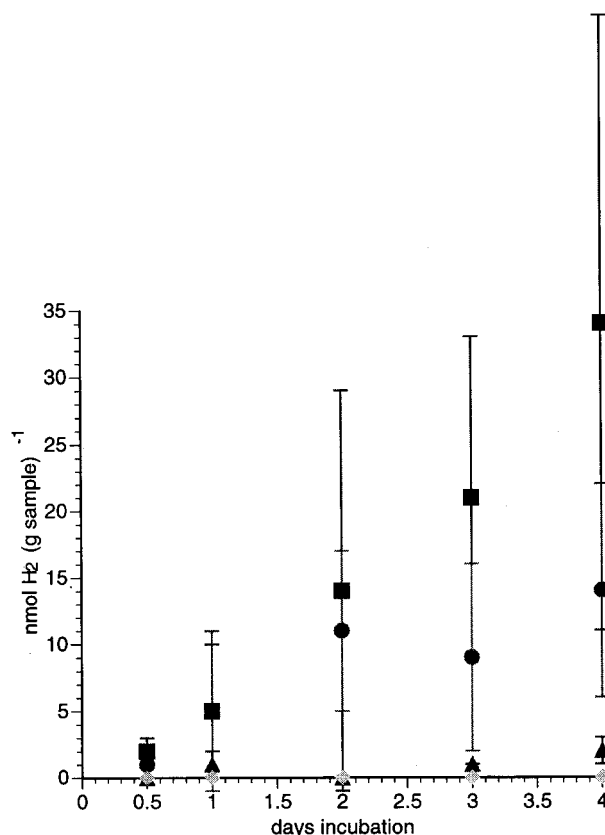


FIGURE 1. H₂ production from individual mineral phases found in basalt. (■) fayalite; (●) forsterite; (▲) augite; (◆) labradorite. Error bars are \pm SD of four samples. These experiments were conducted in 25 mM, pH 6, PIPES buffer in which strong H₂ evolution occurred from most basalt samples. Note that while values for augite appear low, as compared with olivine minerals, the day 4 value corresponds to ca. 1 μ M H₂, while labradorite values remain near 1 nM, similar to quartz or unwetted controls (not shown).

radiorite, (Ca_{0.5}Na_{0.5})(Al_{0.5}Si_{0.5})AlSi₂O₈. The compositions of these minerals in nature vary further due to the incorporation of other elements and also by crystallographic substitution. (For a more detailed description of the mineralogy and chemistry of these minerals, see ref 37.) The measured compositions of the major basalt minerals labradorite, augite, fayalite, and forsterite are shown in Table 1, and the results of corresponding H₂-generation experiments using them are shown in Figure 1. A number of minor ferrous minerals found in basalts (again, as mineral specimens) were also tested but did not produce detectable concentrations of H₂ (data not shown); these included magnetite (Fe₃O₄), ilmenite (FeTiO₃), hematite (Fe₂O₃, a ferric oxide), pyrite (FeS₂), and pyrrhotite (FeS). We also tested two ferrous iron-bearing silicate minerals found in, for example, granitic rocks. Traces of H₂ but no reproducible accumulations were sometimes observed in tests of hornblende [NaCa₂(Mg,Fe,Al)₅(Si,Al)₈O₂₂(OH)₂] and

biotite [K(Mg,Fe)₃(AlSi₃O₁₀)(OH)₂]. The results demonstrated that the ferrous silicate minerals (i.e., pyroxene and olivine) were the primary phases responsible for H₂ production from basalts and suggested that Fe(II) was a key reactant in the H₂-generating reaction. The main ferrous silicates in our standard RUC basalt sample were pyroxenes, largely augite, somewhat richer in Fe (15–16 wt % FeO) than the sample in Table 1, and lesser amounts of pigeonite (21–24 wt % FeO) (36).

Preliminary experiments with RUC basalt in unbuffered solutions generated variable results, accompanied by increasing alkalinity, and suggested that maximal H₂ production occurred near pH 6, yet the in situ pH of the CRB aquifers ranges from 7 to 10 (33). We conducted experiments in 25 mM buffers to determine the control of pH on H₂ production from RUC basalt. As shown in Figure 2, H₂ production rates were dependent on pH, generally increasing with acidity, but H₂ was produced throughout the pH range of the CRB aquifers. H₂ was consistently elevated at pH 11, as compared to pH 9 and pH 10, which is consistent with greater solubility of silicates at pH above 10 and the enhanced dissolution of the rock matrix. At alkaline pH, a lag time preceded the onset of H₂ production, suggesting that some poisoning of the system by water–rock interactions was required to achieve H₂-producing conditions. The pH of solutions remained constant when 25 mM buffers were used, and thus the onset of H₂ production in alkaline experiments did not reflect a change in pH. The standard deviation of the data consistently increased greatly with time in high H₂-producing treatments, regardless of pH or other experimental variables. This is not easily explained by variation in initial conditions (e.g., experimental setup), and its cause remains unknown. Rates of H₂ production were also dependent on temperature and were approximately twice as fast, for most pH values, at 60 °C as they were at 30 °C. The temperature in the CRB can be described by T (°C) = (0.0388)[m depth] + 15.03, so significant variation in H₂ production might be expected over the depth of the formation, which averages 1 km but can reach 3.5 km. The experimental values cover the range of in situ conditions for most of the samples reported in ref 8. Thus, H₂ can be produced from water–basalt interactions at all temperatures and pH values known for CRB aquifers.

During experiments with crushed basalt, particularly at alkaline pH, a variable lag time of 1–3 days often preceded H₂ production. We measured dissolved Fe²⁺ in the reaction mixtures with RUC basalt and noted that the onset of H₂ production appeared to coincide with the appearance of Fe²⁺ in solution. Possible explanations for this included the following: dissolved ferrous ion was a reactant in the H₂-producing reaction, both H₂ and Fe²⁺ were products of dissolution of the rock matrix, or redox poisoning by Fe²⁺ was necessary to enable the H₂-producing reaction. Redox poisoning with 1 mM sulfide or thioglycolate did not stimulate H₂ production (data not shown) and resulted in ca. 2 days longer lag time. Since sulfide forms strong complexes with iron, we tested buffers composed of the iron-complexing anions bicarbonate and phosphate and found that both appeared to cause extension of the lag time before H₂ production, as compared with PIPES buffer. This temporary inhibition of H₂ production could be relieved by adding excess ferrous chloride to the solution. This result suggested in turn that free ferrous ion may have played a role independent of redox buffering. However, H₂ was not produced in quartz controls containing FeCl₂ without basalt.

Since mineral dissolution may be relatively slow, in moderately alkaline solutions, we performed another experiment to determine whether the alkaline inhibitory effect, noted above, was potentially caused by a slowing of mineral dissolution and Fe²⁺ liberation (Figure 3). When the solution was supplemented with 1 mM ferrous chloride, H₂ production

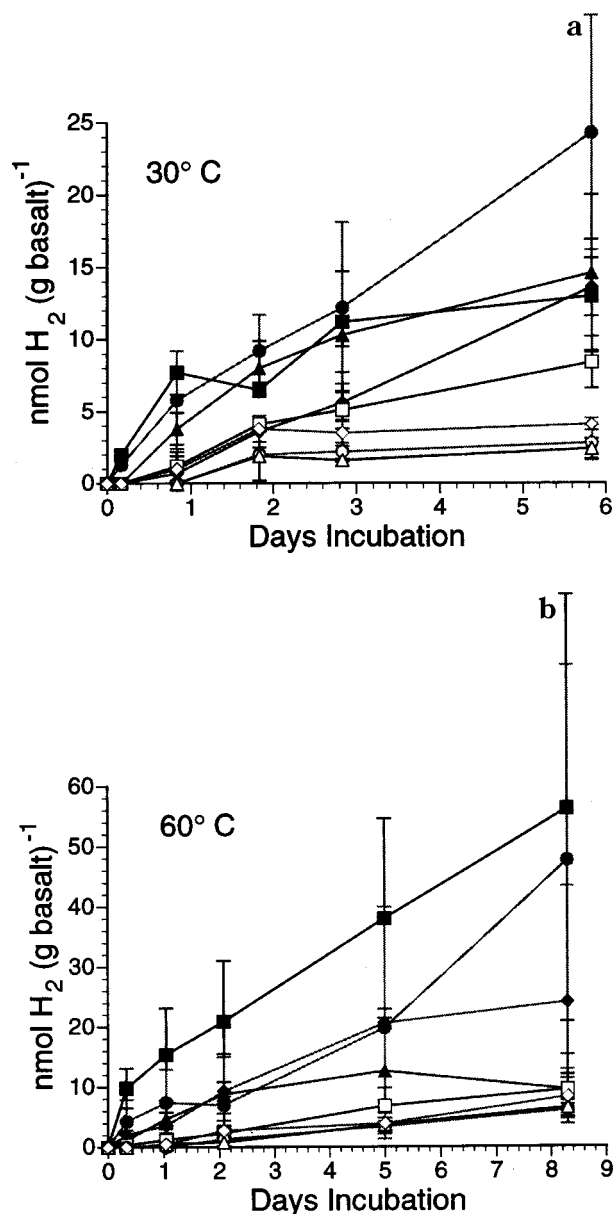


FIGURE 2. H_2 production from RUC basalt as a function of pH and temperature. (a) Reactions at 30 °C. (b) Reactions at 60 °C. 5-g aliquots of milled, autoclaved basalt were placed in sealed pressure tubes under purified N_2 with 5 mL of anaerobic buffer: (■) PIPES pH 5; (●) PIPES pH 6; (▲) PIPES, pH 7; (◆) borax, pH 7; (□) borax, pH 8; (○) borax, pH 9; (△) Borax, pH 10; (◇) borax, pH 11. Four replicate tubes were sampled at each time point, without replacement. Bars are \pm SD ($n = 4$).

was similar at both pH 6 and pH 8. In control experiments, H_2 was not produced from FeCl_2 without basalt (data not shown.) A likely explanation is that added Fe^{2+} poised the system at a lower redox potential by removing residual O_2 ; however, we cannot rule out possible reactions involving both aqueous Fe^{2+} and solid-phase reactants [Fe(II)]. The reduction potential of solid-phase Fe(II), effective through heterogeneous electron transfer at the solid–solution interface, has been hypothesized to be enhanced over that of aqueous Fe^{2+} alone (38). Surface Fe(II), including adsorbed Fe^{2+} , may thus participate in the overall H_2 -producing reaction and may enhance the ability of basalt to reduce H_2O over what would be expected from the considerations of aqueous chemistry alone. Concentrations of Fe^{2+} in deep CRB groundwaters typically range from 10 μM to 1.9 mM (33). The apparent inhibition of H_2 production at alkaline

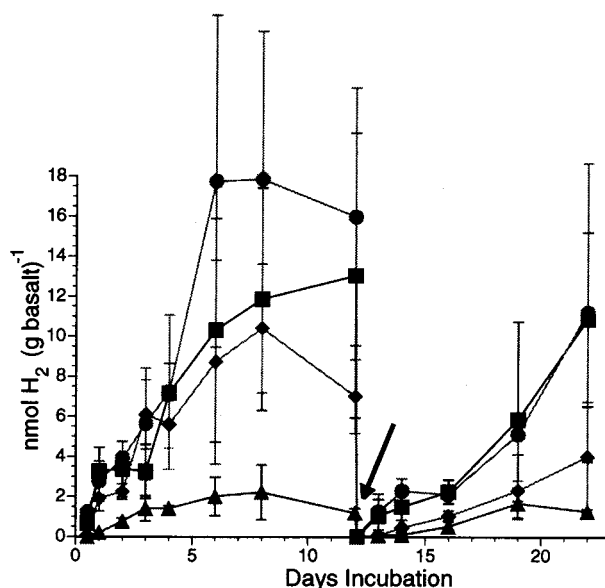


FIGURE 3. H_2 production from RUC basalt at different pH and Fe(II) concentrations. 5-g aliquots of milled, autoclaved basalt were placed in sealed pressure tubes under purified N_2 with 5 mL of anaerobic buffer: (■) 25 mM PIPES, pH 6; (●) 25 mM PIPES + 1 mM FeCl_2 , pH 6; (▲) 25 mM borax, pH 8; (◆) 25 mM borax + 1 mM FeCl_2 , pH 8. Four replicate tubes were sampled at each time point, without replacement. Bars are \pm SD ($n = 4$). On day 12 (arrow), all headspaces were flushed with N_2 to reset the experiment.

conditions may thus have been an artifact of microcosm preparation, i.e., residual sorbed O_2 . No residual O_2 would be present in deep in situ CRB groundwaters.

After several days, H_2 production in our closed experimental systems declined or stopped. Two experiments were conducted to determine whether some ephemeral reactant was depleted, whether H_2 production was kinetically limited by product accumulation, and thus, whether mechanisms that remove H_2 from solution, such as microbial metabolism, could enhance total production. In one experiment, basalt samples were incubated with and without headspace. Since H_2 is poorly soluble, partitioning to the headspace would effectively remove product H_2 from the reacting system. Two sets of five replicate tubes were incubated at 30 °C, as above, with 10 g of RUC basalt and 30 mL of anoxic pH 7 PIPES buffer. In one set, the tubes were filled completely leaving no headspace, and in the other set the same volume was incubated in somewhat larger tubes with a 25-mL headspace of H_2 - and O_2 -free N_2 . Dissolved H_2 in headspace-free tubes was sampled by displacing 5 mL of buffer with N_2 at room pressure and shaking vigorously for 1 min. After 4 days incubation, the tubes without headspace had produced 16 (± 3) nmol of H_2 , while the tubes with headspace had produced 36 (± 9) nmol of H_2 . In addition, after H_2 production had ceased in the Fe-supplementation experiment (Figure 3), the experiment was reset by refilling the headspace of all tubes with purified N_2 while agitating the samples. As shown, this caused H_2 production to begin again. Thus, the H_2 that we observed was not merely released from a trapped reservoir, and concentrations found in the experiments were not controlled by depletion of an ephemeral reactant. Solution H_2 concentrations were subject to kinetic control by product inhibition, and consumption or removal of H_2 from solution could enhance total H_2 production.

Most of our experiments were conducted with sterilized basalt to avoid complications such as consumption of H_2 by microorganisms. Both autoclaving and dry heat baking were effective sterilization methods. Both methods reduced H_2 production over 14 day incubations, as compared to un-

sterilized basalt. However, baking at 200 °C in air (ca. 20% O₂) resulted in about 10-fold less H₂ production than autoclaving at 121 °C in a steam atmosphere (ca. 100% H₂O). When fresh surfaces were generated by remilling the sterilized basalt, H₂ production from both remilled treatments was the same as from the initial autoclaved treatment. This greater inhibition under the more oxidizing sterilization conditions further suggested that redox reactions at mineral surfaces were involved in H₂ production and showed that our microcosm results were conservative relative to in situ conditions.

The results presented here suggest that H₂ is produced in CRB aquifers by the reaction of water with reduced iron minerals at moderate temperatures. This is analogous to the field observations of H₂ production during the serpentinization of ultramafic rocks. Our results do not rule out in situ contributions from some of the other mechanisms listed above, but they are unlikely to have contributed H₂ to our experiments. Any gases produced during or shortly after rock fracturing would be ephemeral and would have been removed during sample processing. Furthermore, the lack of H₂ production from labradorite suggests that iron redox reactions were involved. (It is worth noting that ongoing in situ fracturing of the CRB flows, caused by tectonic processes, could enhance H₂ production by all of the reactive rock processes.) The samples contained no significant amount of organic matter and were sterilized, so fermentation could not have been a source of H₂. Similarly, fermentation of organic matter is unlikely to be the source of H₂ in CRB aquifers (8, 35). The features of our laboratory experiments that are substantively different from in situ basalt aquifers are the large experimental reactive surface area per unit mass (though high surface area volcanic ash beds are present in the CRB), strong pH buffering (although at values covering the in situ range), and the lack of flow through the system. We hypothesize that these laboratory artifacts are compensated in the field by long reaction times characteristic of aged groundwaters, by the potentially large ratio of basalt surface to groundwater volume, and by quasi-steady-state conditions allowed by groundwater flow.

Results reported here and elsewhere (8, 21), along with theoretical modeling results (e.g., ref 39), demonstrate that water–rock interactions are a feasible source of H₂ in basaltic aquifers and that methane in CRB aquifers is formed by microbial CO₂ reduction coupled to H₂. Our hypothesis that these two processes are directly linked in situ remains to be proven; however, the hypothesis is consistent with all existing data.

Extrapolation of these laboratory experiments to derive reaction rates in nature is probably of limited value since the necessary parameters are not known with reasonable confidence. Nevertheless, we offer the following exercise, which should be treated with due skepticism. Groundwater permeates the CRB through a fracture-flow system. Intraflow fracture width in the CRB has been found to follow a log-normal distribution with a mean of 0.14 mm (40) or a surface area of ca. 7.14 m² (L void)⁻¹. In general, as CRB groundwater ages approach 3 × 10⁴ years, based on ¹⁴C extinction (41), methane concentrations approach 100 mM (8, 33), suggesting a production rate of ca. 9.13 nmol L⁻¹ day⁻¹. Considering the stoichiometry of methanogenesis (4H₂ + CO₂ = CH₄ + 2H₂O), this would require 36.5 nmol of H₂ L⁻¹ day⁻¹, or roughly 5 nmol of H₂ (m² of basalt)⁻¹ day⁻¹. This is in surprisingly good agreement with our experimentally measured values, which ranged over ca. 1–6 nmol of H₂ (m² of basalt)⁻¹ day⁻¹ depending on temperature, pH, and dissolved Fe(II). However, the CRB is not homogeneous. Individual basalt flows vary in composition and H₂-generating potential. Most groundwater flows through more permeable interflow areas, which may have much more variable geometry—measure-

ments of hydraulic conductivity vary by 9 orders of magnitude (41). Groundwater age increases with depth and consequently with temperature, so that reaction rates might increase along a flow path (Figure 2). Petrographic studies show that a zone of alteration extends several millimeters into the rock matrix from fracture surfaces (42), suggesting that the effective surface area may be much larger and the specific rates much lower than estimated. Thus, estimating a single rate for the system is certainly an oversimplification. Nevertheless, to a first approximation, it appears feasible that water–rock reactions provide sufficient H₂ to support production of the observed concentration of CH₄ by microorganisms in the CRB.

While our experiments have focused on the CRB system, we know of no reason these phenomena should be unique to this formation. It seems likely that H₂-yielding water–rock reactions may contribute to productivity in many anoxic ecosystems that contain igneous rocks.

Acknowledgments

We gratefully acknowledge the assistance of Bethany Bowling, Alyssa Gall, Aaron Hall, Nicholas Landau, Michael Meyer, Frank Wobber, James Fredrickson, and three anonymous reviewers. This research was supported by the DOE Office of Biological and Environmental Research and the NASA Office of Space Science. Pacific Northwest National Laboratory is operated for DOE by Battelle Memorial Institute under Contract DE-AC06-76RLO 1830.

Literature Cited

- (1) Barnes, I.; Rapp, J. B.; O'Neil, J. R.; Sheppard, R. A.; Gude, A. J., III. *Contrib. Mineral. Petrol.* **1972**, *35*, 26.
- (2) Neal, C.; Stanger, G. *Earth Planet. Sci. Lett.* **1983**, *66*, 315.
- (3) Shcherbakov, A. V.; Kozlova, N. D. *Geotectonics* **1986**, *20*, 120.
- (4) Angino, E. E.; Zeller, E. J.; Dreschhoff, G. A. M. In *Geochemistry of Gaseous Elements and Compounds*; Durrance, E. M., et al., Eds.; Theophrastus Publications: Athens, Greece, 1990; p 486.
- (5) Coveney, R. M., Jr.; Goebel, E. D.; Zeller, E. J.; Dreschhoff, G. A. M.; Angino, E. E. *Am. Assoc. Petrol. Geol. Bull.* **1987**, *71*, 39.
- (6) Abrajano, T.; et al. *Appl. Geochem.* **1990**, *5*, 625.
- (7) Sherwood-Lollar, B.; Frapre, S. K.; Weise, S. M.; Fritz, P.; Macko, S. A.; Welhan, J. A. *Geochim. Cosmochim. Acta* **1993**, *57*, 5087.
- (8) Stevens, T. O.; McKinley, J. P. *Science* **1995**, *270*, 450.
- (9) Schink, B. In *Biology of Anaerobic Microorganisms*; Zehnder, A. J. B., Ed.; Wiley & Sons: New York, 1988; pp 771–846.
- (10) Zehnder, A. J. B., Ed. *Biology of Anaerobic Microorganisms*; Wiley & Sons: New York, 1988.
- (11) Stevens, T. O.; McKinley, J. P.; Fredrickson, J. K. *Microb. Ecol.* **1993**, *25*, 35.
- (12) Kotelnikova, S.; Pedersen, K. *FEMS Microbiol. Ecol.* **1998**, *26*, 121.
- (13) Jannasch, H. W. In *Seafloor Hydrothermal Systems*; Humphris, S. E., et al., Eds.; American Geophysical Union: Washington, DC, 1995; pp 273–296.
- (14) Stevens, T. O. *FEMS Microbiol. Rev.* **1997**, *20*, 327.
- (15) Boston, P. J.; Ivanov, M. V.; McKay, C. P. *Icarus* **1992**, *95*, 300.
- (16) Sleep, N. H.; Zahnle, K. J. *Geophys. Res.* **1998**, *103*, 28529.
- (17) Dolfing, J.; Beurskens, J. E. M. *Adv. Microb. Ecol.* **1995**, *14*, 143.
- (18) Murray, W. D.; Richardson, M. *Crit. Rev. Environ. Sci. Technol.* **1993**, *23*, 195.
- (19) Nealson, K. H.; Saffarini, D. *Annu. Rev. Microbiol.* **1994**, *48*, 311.
- (20) Lovley, D. R. *Annu. Rev. Microbiol.* **1993**, *47*, 263.
- (21) Bjornstad, B. N.; McKinley, J. P.; Stevens, T. O.; Rawson, S. A.; Fredrickson, J. K.; Long, P. E. *Ground Water Monit. Rem.* **1994**, *14*, 140.
- (22) Alt, J. C. In *Seafloor Hydrothermal Systems*; Humphris, S. E., et al., Eds.; American Geophysical Union: Washington, DC, 1995; pp 85–114.
- (23) Arnorsson, S. J. *Geophys. Res.* **1986**, *91*, 12261.
- (24) Apps, J. A.; van de Kamp, P. C. *The Future of Energy Gases*; U.S. Geological Survey Professional Paper 1570; U.S. Geological Survey: Reston, VA, 1993.
- (25) O'Hanley, D. S. *Serpentinities Records of Tectonic and Petrological History*; Oxford University Press: New York, 1996.

- (26) Kelley, D. S. *J. Geophys. Res.* **1996**, *101*, 2943.
- (27) Kita, I.; Masuo, S.; Wakita, A. *J. Geophys. Res.* **1982**, *87*, 10789.
- (28) Freund, F. *Oil Gas J.* **1984**, *82*, 140.
- (29) Mormile, M. R.; Gurijala, K. R.; Robinson, J. A.; McInerney, M. J.; Sufliata, J. M. *Appl. Environ. Microbiol.* **1996**, *62*, 1583.
- (30) Smolenski, W. J.; Robinson, J. A. *FEMS Microbiol. Ecol.* **1988**, *53*, 95.
- (31) Robinson, J. A.; Tiedje, J. M. *Appl. Environ. Microbiol.* **1982**, *44*, 1374.
- (32) Ulf-Moller, F. *Geochim. Cosmochim. Acta* **1990**, *54*, 57.
- (33) Early, T. O.; Spice, G. D.; Mitchell, M. D. *A Hydrochemical Data Base for the Hanford Site, Washington*; RHO-SD-BWI-DP-061; U.S. Department of Energy: Richland, WA, 1986.
- (34) Anderson, R. T.; Chapelle, F. H.; Lovley, D. R. *Science* **1998**, *281*, 976.
- (35) Stevens, T. O.; McKinley, J. P. *Science* **1996**, *272*, 897.
- (36) Allen, C. C.; Johnston, R. G.; Strobe, M. B. *Characterization of reference Umtanum and Cohasset Basalt*; SD-BWI-DP-05; U.S. Department of Energy: Richland, WA, 1985.
- (37) Deer, W. A.; Howie, R. A.; Zussman, J. *An introduction to the rock-forming minerals*, 2nd ed.; Addison-Wesley: Reading, MA, 1992.
- (38) White, A. F.; Yee, A. *Geochim. Cosmochim. Acta* **1985**, *49*, 1263.
- (39) Treiman, A.; Wallendahl, A. *Science* **1998**, *282*, 2196.
- (40) Lindberg, J. W. In *Volcanism and Tectonism in the Columbia River Flood-Basalt Province*; Reidel, S. P., Hooper, P. R., Eds.; Special Paper 239; Geological Society of America: Boulder, CO, 1989; pp 169–186.
- (41) U.S. Department of Energy. *Consultation Draft, Site Characterization Plan, Reference Repository Location, Hanford Site, Washington*; DOE/RW-0164; U.S. Department of Energy: Washington, DC, 1988.
- (42) McKinley, J. P.; Stevens, T. O.; Westall, F. *Geomicrobiol. J.* **2000**, *17*, 1.

Received for review May 24, 1999. Revised manuscript received December 1, 1999. Accepted December 7, 1999.

ES990583G